“Theoretical calculation of uncertainty region based on the general size distribution in the preparation of standard refe rence particles for particle size measurement”

Hideto YOSHIDA*, Tetsuya YAMAMOTO* ,
Kunihiro FUKUI* and Hiroaki MASUDA**

* Department of Chemical Engineering, Hiroshima University, 1-4-1, Kagamiyama Higashi-hiroshima, Hiroshima, 739-8527, Japan

** Professor Emeritus, Kyoto University, Invited Special Research Fellow, Cooperative Research Center of Life Science, Kobe gakuin University, Minatojima, Chuou-ku, Kobe 650-8586, Japan

Corresponding author: Hideto Yoshida
Department of Chemical Engineering, Hiroshima University, 1-4-1, Kagamiyama Higashi-hiroshima, Hiroshima, 739-8527, Japan
Tel. & FAX 082-424-7853, e-mail: r736619@hiroshima-u.ac.jp

Key Words : Particle size, Standard reference particles, Truncated log-normal distribution, Uncertainty region, Size measurement,

Abstract

In order to confirm the reliability of particle size measurement technique and to prepare standard reference particles for calibrating particle size measurement devices, experimental and theoretical studies have been conducted about the uncertainty region of particle size measurement for the general particle size distribution. A new theoretical equation to calculate fundamental uncertainty region in the case that the maximum and minimum particle sizes are known, is derived based on Tschebyscheff theory. The uncertainty regions calculated based on the proposed method are applied to poly-disperse particles and a picket-fence distribution composed of two kinds of nearly mono-disperse particles.

For the poly-disperse particles, the uncertainty region increases with the increase in particle diameter. For the picket-fence distribution composed of two kinds of nearly mono-disperse particles, the uncertainty region increases around the intermediate particle diameters between the two kinds of particles.

Numerical simulation of uncertainty region for the picket-fence distribution has also been carried out. The uncertainty region decreases with the increase in sample size or the decrease in geometric standard deviation.

1. Introduction

Particle size distribution is measured by various methods such as microscopic method, laser diffraction and scattering method, dynamic light scattering method, electrical sensing zone method and liquid sedimentation method. Though the laser diffraction and scattering method, dynamic light scattering method and electrical sensing zone method have the advantage of shorter measurement time and good repeatability, they need complicated calibration by direct method, because these methods are number based measurements. In order to calibrate such particle size measurement devices in mass basis, it is necessary to prepare standard reference particles. As for the reference particles, spherical particles having a size range appropriate to the resolution of the measurement technique are preferable. Yoshida et al. studied on the particle size distributions of three kinds of poly-disperse spherical glass beads (MBP1-10, MBP3-30, MBP10-100) based both on improved type sedimentation balance method (mass base measurement) and microscopic method (number base measurement) with sample size larger than 10000 particles (1, 2). These reference particles are ranged from 1 μm to 10μm, 3 μm to 30 μm, and 10 μm to 100 μm, respectively. Round robin tests are also carried out on the two kinds of spherical particles (MBP1-10, MBP10-100), and the results are reported by Mori et al. (3).

In order to represent particle size distribution obtained by

microscopic method, uncertainty region of the mass base distribution should be calculated. On this purpose, Masuda et al. derived analytical equation to calculate the necessary sample size under known fundamental uncertainty region and vice versa (4, 5). However, the original theory is thought to be applied only for the log-normal distribution.

In the real microscopic counting process, the data of particle size distribution with the maximum and minimum size for the general particle size distribution is usually obtained. In such a case, the uncertainty region of the general size distribution should be considered, but this problem has not been clearly solved.

This paper presents a new equation to estimate the uncertainty region of the general size distribution in the case that the maximum and minimum particle sizes are known. And the equation is applied to the two cases; (1) poly-disperse particles and (2) picket-fence size distribution composed of two kinds of nearly mono-disperse particles. The numerical simulation is also carried out to examine the reliability of the proposed new model. The method proposed may be applied to the uncertainty estimation of particle size distribution for the reference particles.

2 Measurement of particle size distribution by microscopic method

Measurement of particle size distribution was carried out for the spherical glass particles. Figure 1 shows a photograph of the particles taken by scanning microscope (SEM S-2400, Hitachi, Co., Ltd.). The magnification was set to 500. Based on the SEM photographs, the particle size was measured manually by marking a suitable sized circle on each particle. In order to eliminate counting error near the frame border-line, size measurement was carried out only to the particles having the center positions inside the screen based on ISO 13322-1. The total sample size was 39,500 and particle size distribution ranges from 3 to 30μm. Obtained data of the size distribution is shown in Table 1 and Fig.2. Details of the counting procedure are indicated in our previous paper (6). Horizontal bars shown in the figure will be explained later.

3 Estimation of uncertainty region for the general size distribution

In order to estimate the uncertainty region for the general size distribution, it is necessary to obtain the relationship between cumulative distribution based on volume and that based on count. The data of general particle size distribution obtained by use of the microscope is shown in Table 2. For the particle diameter from x_i to x_{i+1}, n_i particles are detected among the total sample size of N. The frequency distributions based on number and volume are indicated as $q_{0,i}\Delta x_i$ and $q_{3,i}\Delta x_i$, respectively. The

cumulative distribution based on number in this size range i is as follows:

$$Q_{0,i} = \frac{n_1 + n_2 + --+n_i}{n_1 + n_2 + --+n_n} = \frac{x_1{}^0 n_1 + x_2{}^0 n_2 + --+x_i{}^0 n_i}{x_1{}^0 n_1 + x_2{}^0 n_2 + --+x_n{}^0 n_n} \qquad (1)$$

The uncertainty region for the size range i is given by Eq.(2) based on ISO-14488.

$$\delta Q_{0,\mathrm{i}} = u \sqrt{\frac{Q_{0,\mathrm{i}}\,(1-Q_{0,\mathrm{i}})}{N}} \qquad (2)$$

where u is the parameter and 1.96 for 95% reliability level.

On the other hand, the cumulative distribution based on volume in the size range i is as follows:

$$Q_{3,i} = \frac{x_1{}^3 n_1 + x_2{}^3 n_2 + --+x_i{}^3 n_i}{x_1{}^3 n_1 + x_2{}^3 n_2 + --+x_n{}^3 n_n} \qquad (3)$$

The value of n_i is shown as the following equations.

$$n_1 = N\,Q_{0,1}, \quad n_2 = N\,(Q_{0,2} - Q_{0,1}), \quad n_3 = N\,(Q_{0,3} - Q_{0,2}),$$
$$n_i = N\,(Q_{0,i} - Q_{0,i-1}), \quad n_n = N\,(Q_{0,n} - Q_{0,n-1}) \qquad (4)$$

Substituting Eq.(4) into Eq.(3), the following equation is obtained.

$$Q_{3,i} = \frac{x_1{}^3 Q_{0,1} + x_2{}^3 (Q_{0,2} - Q_{0,1}) + --+x_i{}^3 (Q_{0,i} - Q_{0,i-1})}{x_1{}^3 Q_{0,1} + x_2{}^3 (Q_{0,2} - Q_{0,1}) + --+x_n{}^3 (Q_{0,n} - Q_{0,n-1})} = \frac{g_i}{g_n} \qquad (5\text{-}1)$$

where,

$$g_i \equiv x_1{}^3 Q_{0,1} + x_2{}^3 (Q_{0,2} - Q_{0,1}) + --+x_i{}^3 (Q_{0,i} - Q_{0,i-1}) \qquad (5\text{-}2)$$

The uncertainty region of the cumulative distribution is calculated as follows:

$$\delta Q_{3,i} = \frac{\partial Q_{3,i}}{\partial Q_{0,1}} \delta Q_{0,1} + \frac{\partial Q_{3,i}}{\partial Q_{0,2}} \delta Q_{0,2} + --+ \frac{\partial Q_{3,i}}{\partial Q_{0,n}} \delta Q_{0,n} \qquad (6)$$

$i > j$ $$\frac{\partial Q_{3,i}}{\partial Q_{0,j}} = \frac{(x_j^{\,3} - x_{j+1}^{\,3})\,(g_n - g_i)}{g_n^{\,2}} \qquad (7\text{-}1)$$

$i=j$ $$\frac{\partial Q_{3,i}}{\partial Q_{0,j}} = \frac{x_j^{\,3} g_n - (x_j^{\,3} - x_{j+1}^{\,3})\,g_i}{g_n^{\,2}} \qquad (7\text{-}2)$$

$i < j$ $$\frac{\partial Q_{3,i}}{\partial Q_{0,j}} = \frac{0 - (x_j^{\,3} - x_{j+1}^{\,3})\,g_i}{g_n^{\,2}} \qquad (7\text{-}3)$$

$i < j,\ j=n$ $$\frac{\partial Q_{3,i}}{\partial Q_{0,j}} = \frac{0 - x_j^{\,3}\,g_i}{g_n^{\,2}} \qquad (7\text{-}4)$$

For the last size region n, substituting $i=n$ into Eq.(5-1), the following equation is obtained.

$$Q_{3,n} = \frac{x_1^{\,3} Q_{0,1} + x_2^{\,3}(Q_{0,2} - Q_{0,1}) + --- + x_n^{\,3}(Q_{0,\mathrm{n}} - Q_{0,n-1})}{x_1^{\,3} Q_{0,1} + x_2^{\,3}(Q_{0,2} - Q_{0,1}) + --- + x_n^{\,3}(Q_{0,n} - Q_{0,n-1})} = \frac{g_n}{g_n} = 1 \qquad (8)$$

Then, each term of Eq.(7) is zero for the last size region.

$$\frac{\partial Q_{3,n}}{\partial Q_{0,j}} = 0 \qquad (j = 1 \sim n) \qquad (9)$$

Substituting Eq.(9) into Eq.(6), the uncertainty region of the last size region is zero.

$$\delta Q_{3,n} = 0 \qquad (10)$$

The maximum uncertainty region for the size range i is obtained as follows:

$$\left|\delta Q_{3,i}\right| \le \left|\frac{\partial Q_{3,i}}{\partial Q_{0,1}}\right| \left|\delta Q_{0,1}\right| + \left|\frac{\partial Q_{3,i}}{\partial Q_{02}}\right| \left|\delta Q_{0,2}\right| + --- + \left|\frac{\partial Q_{3,i}}{\partial Q_{0,n}}\right| \left|\delta Q_{0,n}\right| \qquad (11)$$

In order to calculate $\delta Q_{3,i}$, the evaluation of $\delta Q_{0,1}$ is necessary. For the general size distribution, the uncertainty region is given by the following equation based on Tschebyscheff theory.

$$Q_{0,i}^{\,*} - 4.47\sqrt{\frac{Q_{0,i}^{\,*}(1 - Q_{0,i}^{\,*})}{N}} \le Q_{0,i} \le Q_{0,i}^{\,*} + 4.47\sqrt{\frac{Q_{0,i}^{\,*}(1 - Q_{0,i}^{\,*})}{N}} \qquad (12)$$

where $Q_{0,i}^{\,*}$ indicates the true cumulative distribution on count

base. Therefore, the uncertainty region $|\delta Q_{0,i}|$ is;

$$|\delta Q_{0,i}| = 4.47\sqrt{\frac{Q_{0,i}(1-Q_{0,i})}{N}} \qquad (13)$$

Further, the uncertainty region δx_i of the general distribution for size range i is calculated by the following equation.

$$\delta x_i = \frac{|\delta Q_{3,i}|}{q_{3,i}} \qquad (14)$$

By use of Eqs.(7),(11),(13) and (14), the uncertainty region of particle diameter for the general size distribution is fully determined.

4 Calculation of uncertainty region

4-1 Poly-disperse particles

In order to evaluate the uncertainty region for the general size distribution, calculation was firstly carried out for the poly-disperse particles.

Figure 2 shows the cumulative distribution based on the data of Table 1. The data shows log-normal distribution with mass median diameter $x_{50,3}$=12.8μm and standard deviation s_x=0.405. The solid line indicates the calculated log-normal distribution. The calculated uncertainty region based on the equations obtained in the previous section is also indicated in the figure. The uncertainty region indicated by horizontal bar at several points shows that the uncertainty region increases as the particle

diameter increases. This trend is the same as in our previous paper (6).

4-2 Picket-fence distributions composed of two kinds of nearly mono-disperse particles

In order to calculate the uncertainty region of picket-fence distributions composed of two kinds of nearly mono-disperse particles, a modified size distribution with maximum and minimum particle size based on log-normal distribution is considered.

Figure 3 shows the relationship between cumulative distribution and a parameter g defined by the following equation.

$$g = \frac{\ln x - \ln \bar{x}}{\ln \sigma_g} \qquad (15)$$

The parameters g_0 and g_1 in Fig.3 correspond to the minimum and the maximum particle diameters, respectively. The solid line shows the perfect log-normal distribution and the dotted line indicates the cumulative distribution truncated by the minimum and the maximum particle sizes. The undersize in this case is represented as follows:

$$g < g_0 \qquad Q(g) = 0 \qquad (16\text{-}1)$$

$$g_0 \leqq g \leqq g_1 \qquad Q(g) = \frac{1}{M}\frac{1}{\sqrt{2\pi}}\int_{g_0}^{g} \exp\left(-\frac{\varsigma^2}{2}\right) d\varsigma \qquad (16\text{-}2)$$

$$g > g_1 \qquad Q(g) = 1 \qquad (16\text{-}3)$$

where $$M = M_0 + M_1 = 1 - U_0 - U_2 \qquad (16\text{-}4)$$

Figure 4 shows schematically the corresponding truncated

frequency distribution.

$$g < g_0 \qquad q(g) = 0 \qquad (17\text{-}1)$$

$$g_0 \leqq g \leqq g_1 \qquad q(g) = \frac{1}{M}\frac{1}{\sqrt{2\pi}}\exp\left(-\frac{g^2}{2}\right) \qquad (17\text{-}2)$$

$$g > g_1 \qquad q(g) = 0 \qquad (17\text{-}3)$$

Due to the particle size distribution truncated by the minimum size and the maximum size, M is smaller than unity. In order to calculate the uncertainty region of picket-fence distribution composed of two kinds of nearly mono-disperse particles, the true particle size distribution is represented by the following equations. When the two kinds of nearly mono-disperse particles that follows Eqs.(16),(17) are uniformly mixed with N_1 and N_2 particles, the parameter g and minimum and maximum particle diameters are as follows:

$$g_1 = \frac{\ln x - \ln \bar{x}_{3,1}}{\ln \sigma_{g,1}} \qquad g_2 = \frac{\ln x - \ln \bar{x}_{3,2}}{\ln \sigma_{g,2}} \qquad (18)$$

$$x_{1,\max} = \bar{x}_{3,1}\exp(g_{1,\max}\ln\sigma_{g,1}), \quad x_{1,\min} = \bar{x}_{3,1}\exp(g_{1,\min}\ln\sigma_{g,1}) \qquad (19\text{-}1)$$

$$x_{2,\max} = \bar{x}_{3,2}\exp(g_{2,\max}\ln\sigma_{g,2}), \quad x_{2,\min} = \bar{x}_{3,2}\exp(g_{2,\min}\ln\sigma_{g,2}) \qquad (19\text{-}2)$$

where g_1 and g_2 are the parameter g of particle 1 and 2, respectively. In Eqs.(18) and (19), the mass mediam diameter of particle 1 and 2 are represented by $\bar{x}_{3,1}$ and $\bar{x}_{3,2}$, respectively. In this simulation, it is assumed that the maximum particle diameter of particle 1 is smaller than the minimum particle diameter of particle 2.

$$x_{1,\max} \leq x_{2,\min} \qquad (20)$$

Then, the cumulative distribution and frequency distribution is

represented by the following equations:

$$x < x_{1,\min} \qquad Q_3(g) = 0 \qquad (21\text{-}1)$$

$$x_{1,\min} \leqq x \leqq x_{1,\max} \qquad Q_3(g) = \frac{x_1}{M}\frac{1}{\sqrt{2\pi}}\int_{g_{1,\min}}^{g} \exp\left(-\frac{\varsigma^2}{2}\right)d\varsigma \qquad (21\text{-}2)$$

$$x_{1,\max} < x < x_{2,\min} \qquad Q_3(g) = x_1 \qquad (21\text{-}3)$$

$$x_{2,\min} \leqq x \leqq x_{2,\max} \qquad Q_3(g) = x_1 + \frac{x_2}{M}\frac{1}{\sqrt{2\pi}}\int_{g_{2,\min}}^{g} \exp\left(-\frac{\varsigma^2}{2}\right)d\varsigma \qquad (21\text{-}4)$$

$$x_{2,\max} < x \qquad Q_3(g) = 1 \qquad (21\text{-}5)$$

The frequency distribution is defined as follows:

$$x < x_{1,\min} \qquad q_3(g) = 0 \qquad (21\text{-}6)$$

$$x_{1,\min} \leqq x \leqq x_{1,\max} \qquad q_3(g) = \frac{x_1}{M}\frac{1}{\sqrt{2\pi}}\exp\left(-\frac{g^2}{2}\right) \qquad (21\text{-}7)$$

$$x_{1,\max} < x < x_{2,\min} \qquad q_3(g) = 0 \qquad (21\text{-}8)$$

$$x_{2,\min} \leqq x \leqq x_{2,\max} \qquad q_3(g) = \frac{x_2}{M}\frac{1}{\sqrt{2\pi}}\exp\left(-\frac{g^2}{2}\right) \qquad (21\text{-}9)$$

$$x_{2,\max} < x \qquad q_3(g) = 0 \qquad (21\text{-}10)$$

In the simulation, the following parameter values are used in the calculation.

$$U_0 = 0.01,\ U_2 = 0.01, \qquad \bar{x}_{0,1} = 1\mu\text{m}, \qquad \bar{x}_{0,2} = 3\mu\text{m}$$

The count median diameters of particle 1 and 2 are set to be 1μm and 3μm, respectively.

Case1 Simulation results of $\sigma_g = 1.1$

Figure 5 shows the calculated results of cumulative distribution. In this case, the geometric standard deviation σ_g for each particle is set to be 1.1, and 500 trials are carried out in the calculation. For one trial, the number of particles produced for

the particle 1 and 2 are 2000 and 200, respectively. Although the geometric standard deviation is relatively small, the calculated results indicate the uncertainty region under various constant cumulative distribution values. For each trial, the maximum and minimum particle diameters are determined uniquely, but those diameters obtained do not take the same values. Then, it is found that the value of cumulative distribution $Q_3(x)$ from $x_{1,\max}$ to $x_{2,\min}$ does not show the same constant value for each trial.

Figure 6 shows the calculated results for one trial case. In this case, the uncertainty regions are shown by horizontal bars for several different particle diameters. The uncertainty region becomes fairly wide around $x_{1,\max}$ to $x_{2,\min}$. The reasons considered are as follows:

① The assumption of Eq.(20), $x_{1,\max} < x_{2,\min}$, is used in the simulation, then standard deviation around these regions tends to increase rapidly. The increase of standard deviation increases the uncertainty region in this size range.

② Around the points of $x_{1,\max}$ to $x_{2,\min}$, the cumulative distribution of $Q_{3,i}$ is not indicates a continuous function. Then the values calculated by Eqs.(7-1)-(7-4) indicate relatively large values around these special size range.

For particle diameters from $x_{1,\min}$ to $x_{1,\max}$, the uncertainty region increases with the increase in particle diameter.

Figure 7 shows the calculated results for one trial under the condition of N_1=4000 and N_2=400. Comparing Figs.6 and 7, the

uncertainty region in Fig.7 is smaller than that in Fig.6. This is due to the difference of total sample size between Figs.6 and 7. From Eq.(13), the uncertainty region decreases with the increase in total sample size.

Figure 8 shows the calculated results for one trial under the condition of N_1=6000 and N_2=600. Other calculation conditions are the same as in Figs.6 and 7. Comparing Figs.6,7 and 8, the uncertainty region in Fig.8 is the smallest among the three cases, as the total sample number in Fig.8 is the largest. It is also found that the uncertainty region in any cases increases near the region of particle diameter from $x_{1,\min}$ to $x_{2,\max}$. On the other hand, for one trial case shown in Figs.6,7 and 8, the cumulative value from $x_{1,\min}$ to $x_{2,\max}$ indicates the constant value of mixture ratio of x_1 shown in Eq.(21-3). Figure 9 shows the calculated results for one trial under the following condition:

N_1=3400, N_2=1000

The total sample number in Fig.9 is the same as in Fig.7, but the mixture ratio of each particle is different. The mixture ratio of particle 1 in Fig.9 is smaller than that in Fig.7, then the lower cumulative value about 0.11 in the region of from $x_{1,\min}$ to $x_{2,\max}$ is indicated. The uncertainty region increases as the picket fence property increases. This effect might be the reason of the difference of uncertainty region between the two cases. It is also found that the uncertainty region increases around $x_{1,\max}$ to $x_{2,\min}$.

Case2 Simulation results of σ_g=1.05

Figure 10 shows the calculated results of simulation. The standard deviation for each particle is set to be 1.05, and 500 trials are carried out in the calculation. For one trial, the number of particles produced from the particle 1 and 2 are 2000 and 200, respectively. Comparing Figs.5 and 10, it is found that the uncertainty region decreases in the case of Fig.10, as the geometric standard deviation used is 1.05, that is nearly mono-disperse particles are produced in this simulation. It is also found that value of cumulative distribution $Q_3(x)$ from $x_{1,\min}$ to $x_{2,\max}$ does not show the same constant value for each trial. But the uncertainty region in Fig.10 is relatively smaller than that in Fig.5.

Figure 11 shows the calculated results for one trial under the condition of N_1=2000, N_2=200 and σ_g=1.05.

Comparing Figs.6 and 11, only the standard deviation is different to each other and other calculation conditions are same. Due to the smaller geometric standard deviation, the uncertainty region in Fig.11 is smaller than that in Fig.6. Although the total sample size in Fig.11 is 2200 and this value is smaller than that of 6600 in Fig.8, the uncertainty region is nearly equal for the both cases. It is also found that the uncertainty region increases around the region of particle diameter from $x_{1,\max}$ to $x_{2,\min}$.

The proposed calculation method of uncertainty region might

be applicable to the evaluation of real experimental data for the picket-fence distribution composed of different kinds of nearly mono-disperse particles.

Conclusion

The uncertainty region of the general particle size distribution is theoretically considered and the following conclusions are obtained.

(1) The uncertainty region for the general particle size distribution is derived as Eqs.(6)-(14) by use of Tschebyscheff theory.

(2) For poly-disperse particles, the uncertainty region increases as the particle diameter increases.

(3) For a picket-fence distribution composed of two kinds of nearly mono-disperse particles, the uncertainty region increases around the region from $x_{1,\max}$ to $x_{2,\min}$.

(4) The uncertainty region decreases as the geometric standard deviation decreases or the total sample size increases.

(5) The estimation method proposed here may be applicable to evaluate the uncertainty region for various reference particles.

Nomenclature

g : parameter defined by Eq.(15) (-)

g_i, g_n: parameter defined by Eq.(5) (-)

n_i: sample size in size range i (-)

N : total sample size (-)

Q_0, Q_3 : cumulative distribution based on number and volume, respectively (-)

$Q_{0,i}^{*}$: true cumulative distribution of size range i based on number (-)

q_0, q_3 : size frequency distribution based on number and volume, respectively (-/μm)

x, x_i : particle diameter and particle diameter in size range i (μm)

Δx_i : particle size interval in size range i (μm)

$\bar{x}_{0,i}, \bar{x}_{3,i}$: median diameter of particle i based on number and volume, respectively (μm)

δx_i : uncertainty region of size range i (μm)

M: parameter used in Eq.(16-4) (-)

σ_g: geometric standard deviation (-)

References

[1] Yoshida H., H. Masuda, K. Fukui, and Y. Tokunaga: "Particle size measurement with an improved sedimentation

balance method and microscopic method together with computer simulation of necessary sample size", Advanced Powder Tech., 12, pp.79-94 (2001)

[2] Yoshida H., H. Masuda, K. Fukui, and Y.Tokunaga :"Particle size measurement of standard reference particle candidates with improved size measurement devices", Advanced Powder Tech., 14, pp.17-31 (2003)

[3] Mori,Y., H.Yoshida and H. Masuda :"Characterization of reference particles of transparent glass by laser diffraction method", Particle & Particle Systems Characterization, 24, pp.91-96 (2007)

[4] Masuda,H. and K.Iinoya: "Theoretical study of the scatter of experimental data due to particle size distribution", J.Chem.Eng., Japan, 4, pp.60-67 (1971)

[5] Masuda, H. and K.Gotoh: "Study on the sample size required for the estimation of mean particle diameter", Advanced Powder Technol., 10, pp.159-173 (1999)

[6]Yoshida, H., Y. Mori, H. Masuda and T. Yamamoto: "Particle size measurement of standard reference particle candidates and theoretical estimation of uncertainty region", Advanced Powder Technol., 20, pp.149-149 (2009)

Figure Caption

(N_1=3400, N_2=1000, one trial)

Fig.10 Simulation results of cumulative distribution composed of two kinds of nearly mono-disperse particles
(N_1=2000, N_2=200, 500 trials, σ_g=1.05)

Fig.11 Simulation results of cumulative distribution composed of two kinds of nearly mono-disperse particles
(N_1=2000, N_2=200, one trial, σ_g=1.05)

Table 1　Particle size distribution data

x_{i-1}～x_i[μm]	n_i[−]	q_0[−/μm]	q_3[−/μm]	Q_3[−]
0～1	0	0.000	0.000	0.000
1～2	0	0.000	0.000	0.000
2～3	3	0.000	1.188E-06	1.188E-06
3～4	373	0.009	4.055E-04	4.066E-04
4～5	3000	0.076	0.007	0.007
5～6	5322	0.135	0.022	0.030
6～7	6149	0.156	0.043	0.073
7～8	5686	0.144	0.061	0.133
8～9	4709	0.119	0.073	0.207
9～10	3678	0.093	0.080	0.287
10～11	2858	0.072	0.084	0.371
11～12	2054	0.052	0.079	0.450
12～13	1606	0.041	0.080	0.529
13～14	1103	0.028	0.069	0.598
14～15	780	0.020	0.060	0.658
15～16	592	0.015	0.056	0.714
16～17	445	0.011	0.051	0.765
17～18	325	0.008	0.044	0.809
18～19	241	0.006	0.039	0.848
19～20	177	0.004	0.033	0.881
20～21	114	0.003	0.025	0.906
21～22	94	0.002	0.024	0.930
22～23	59	0.001	0.017	0.947
23～24	57	0.001	0.019	0.965
24～25	39	0.001	0.015	0.980
25～26	14	0.000	0.006	0.986
26～27	7	0.000	0.003	0.989
27～28	5	0.000	0.003	0.992
28～29	5	0.000	0.003	0.995
29～30	0	0.000	0.000	0.995
30～31	0	0.000	0.000	0.995
31～32	2	0.000	0.002	0.996
32～33	1	0.000	0.001	0.997
33～34	0	0.000	0.000	0.997
34～35	0	0.000	0.000	0.997
35～36	0	0.000	0.000	0.997
36～37	0	0.000	0.000	0.997
37～38	1	0.000	0.001	0.999
38～39	1	0.000	0.001	1.000
total	39500	1.000	1.000	

Table 2 Data table of general particle size distribution

size range (μm)	interval (μm)	number (-)	count ratio (-)	mass ratio (-)
x_0-x_1	Δx_1	n_1	$q_{0,1}\Delta x_1$	$q_{3,1}\Delta x_1$
x_1-x_2	Δx_2	n_2	$q_{0,2}\Delta x_2$	$q_{3,2}\Delta x_2$
x_2-x_3	Δx_3	n_3	$q_{0,3}\Delta x_3$	$q_{33}\Delta x_3$
x_{i-1}-x_i	Δx_i	n_i	$q_{0,i}\Delta x_i$	$q_{3,i}\Delta x_i$
x_{n-1}-x_n	Δx_n	n_n	$q_{0,n}\Delta x_n$	$q_{3,n}\Delta x_n$

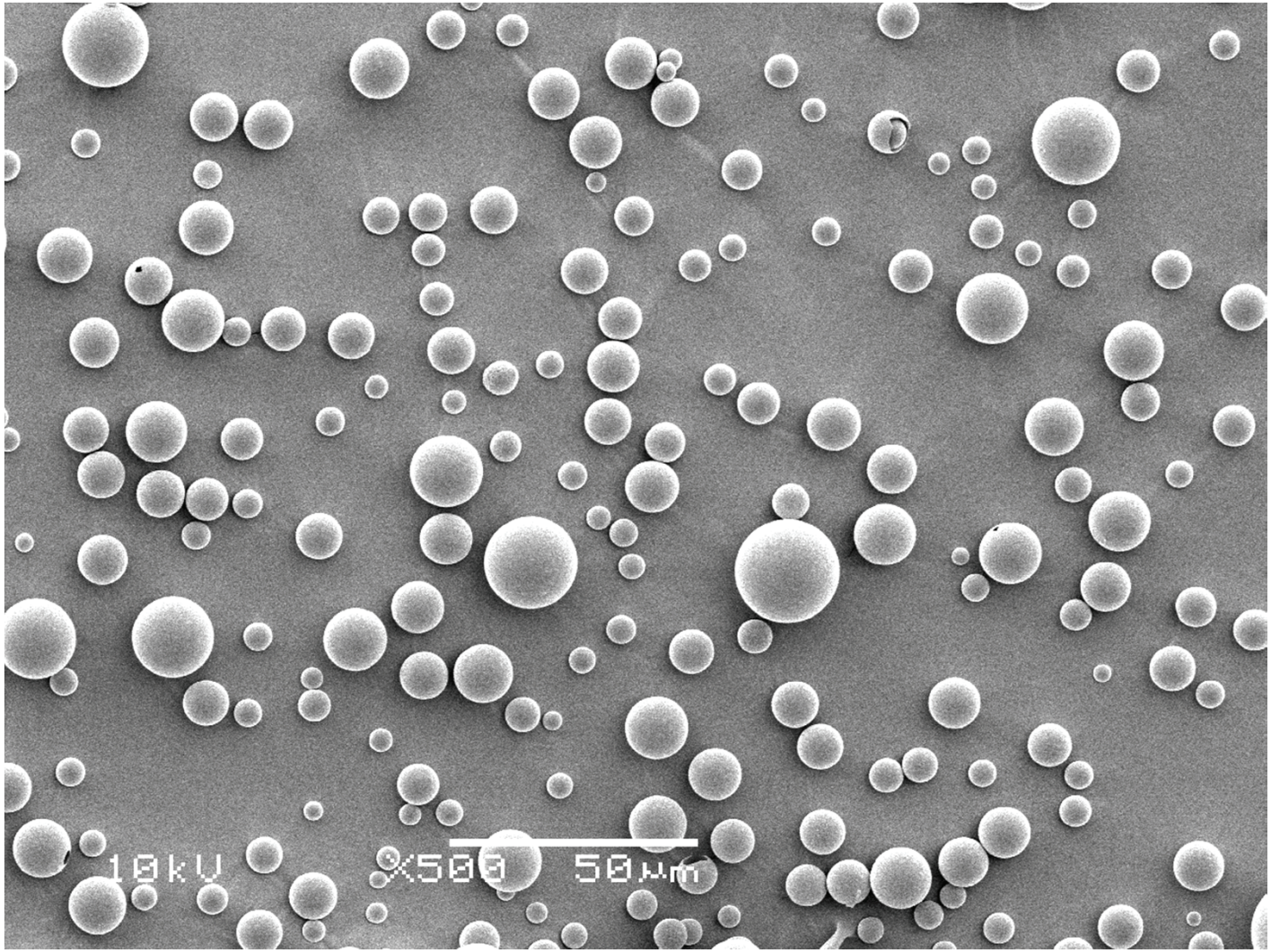

Fig.1 Photograph of reference particle measured by SEM (MBP 3-30)

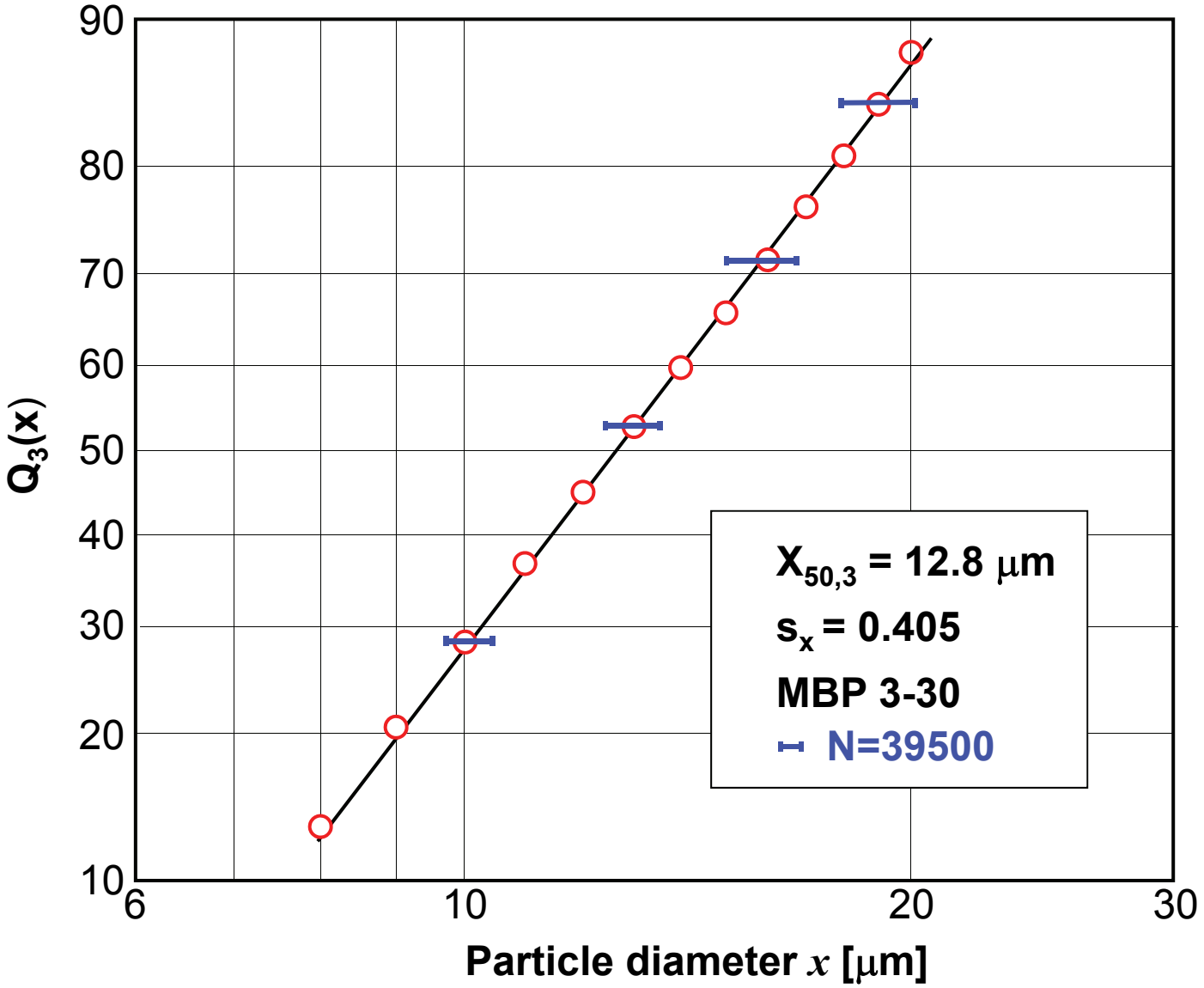

Fig.2 Particle size distribution indicated on log-normal sheet

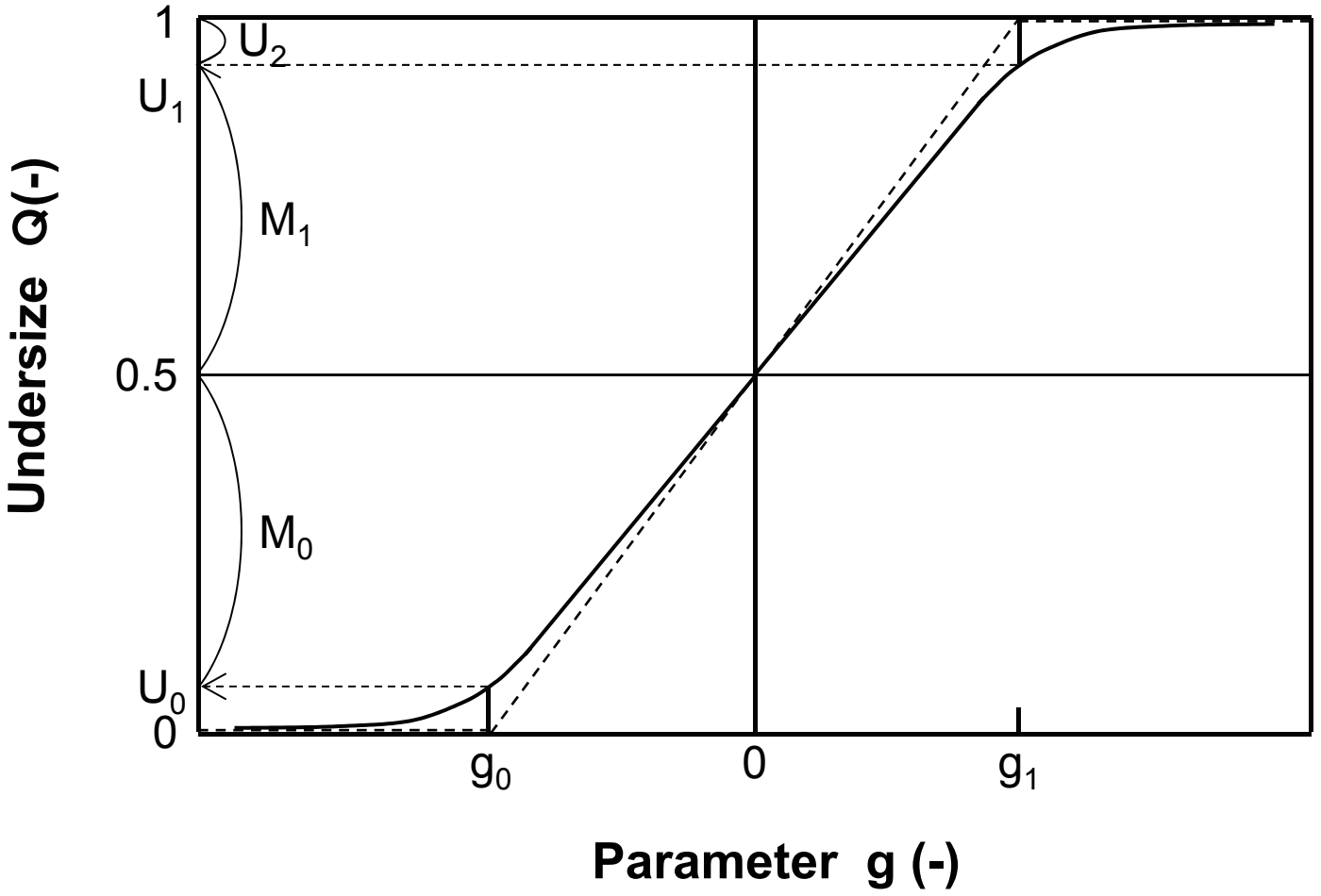

Fig.3 Corrected distribution with known maximum and minimum particle sizes

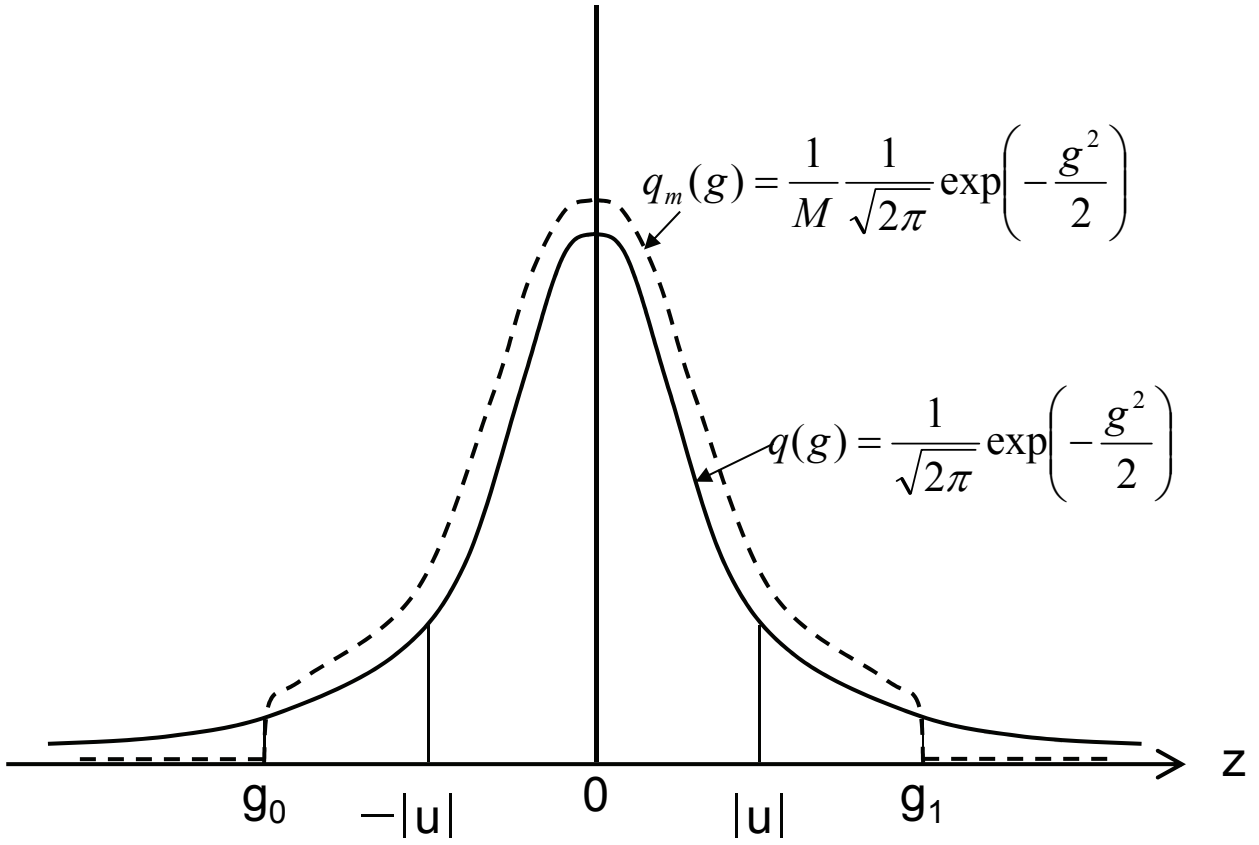

Fig.4 Truncated frequency distribution with known maximum and minimum particle sizes

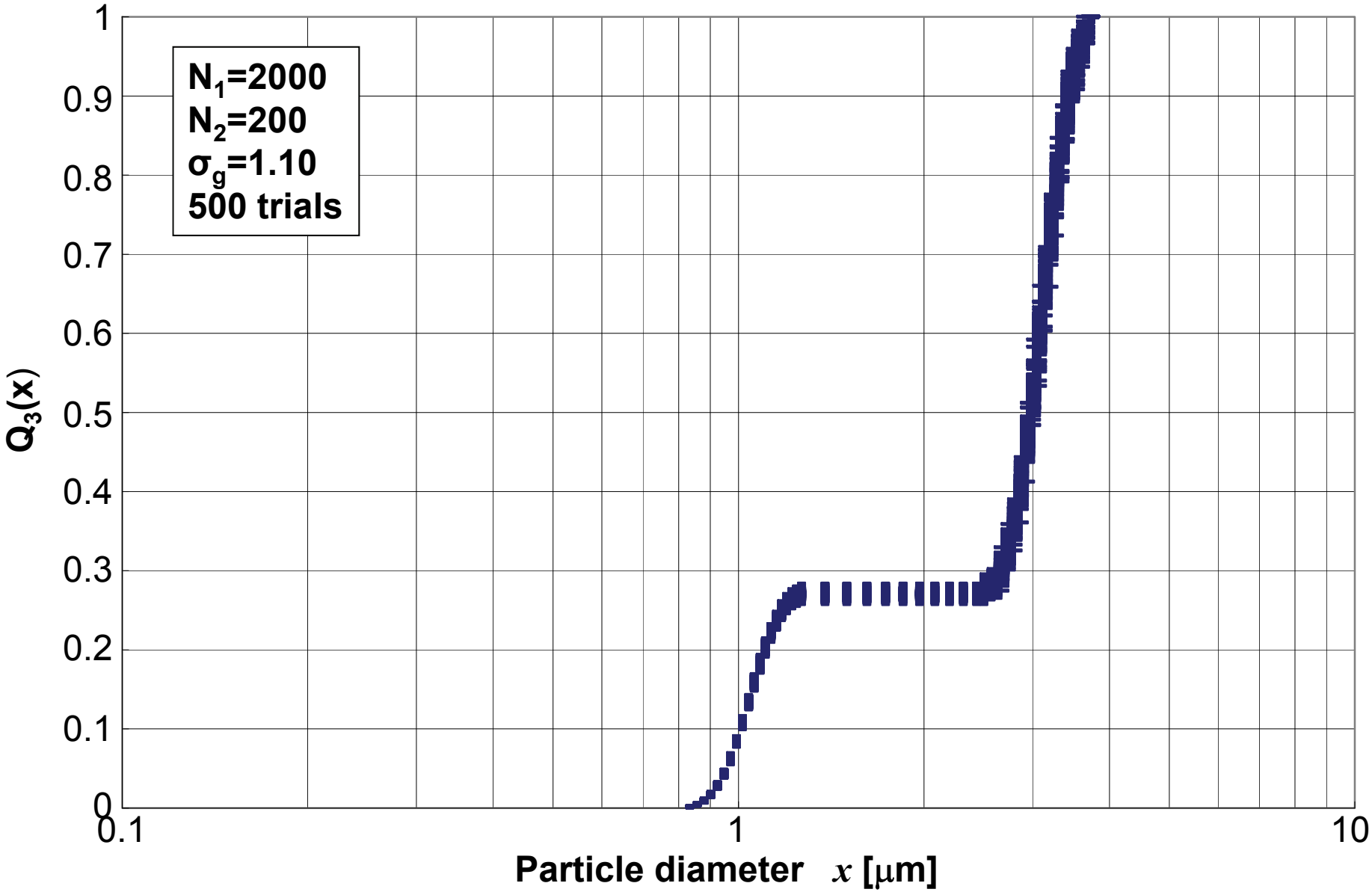

Fig.5 Simulation results of cumulative distribution composed of two kinds of nearly mono-disperse particles (N_1=2000, N_2=200, 500 trials)

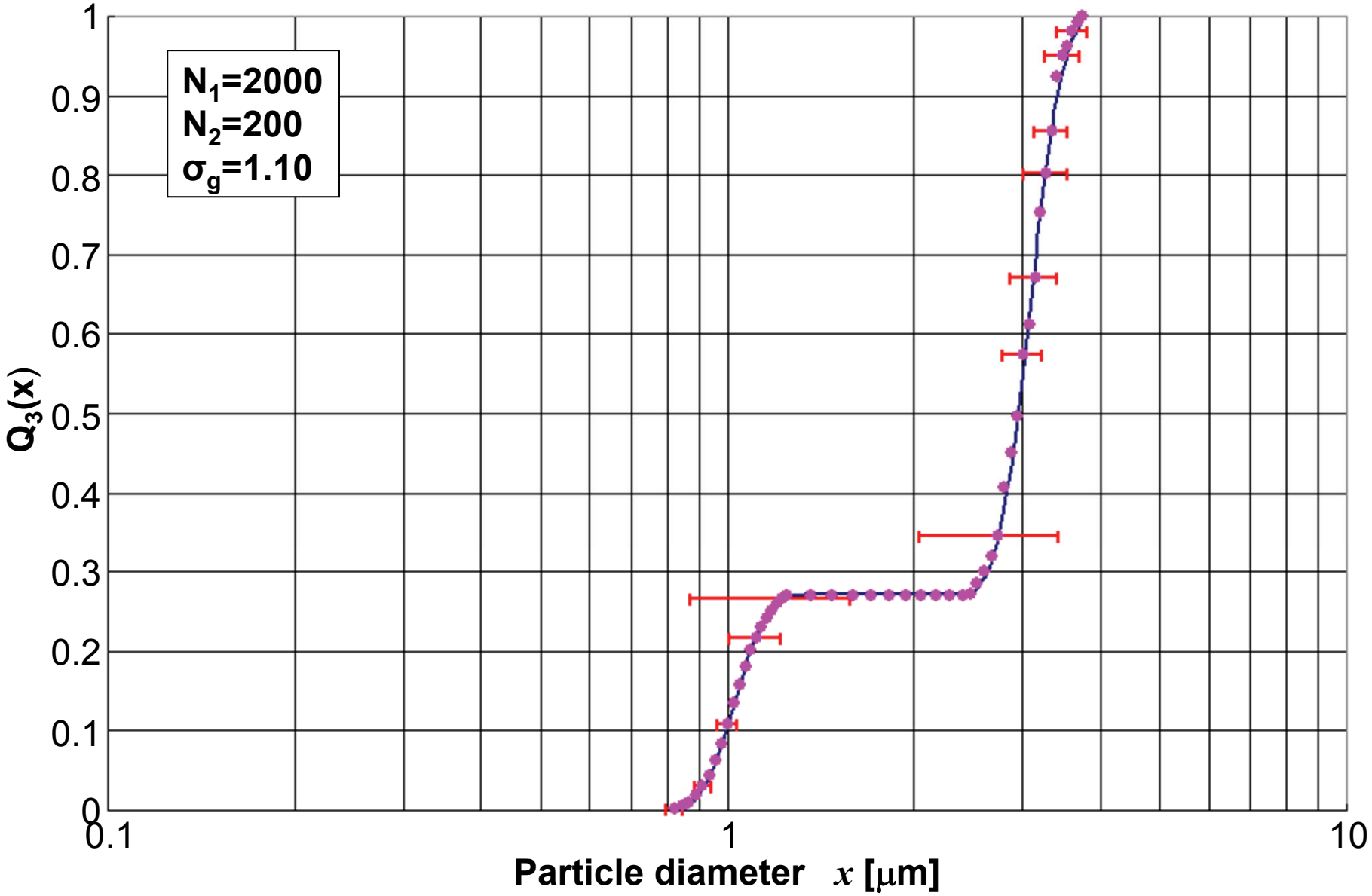

Fig.6 Simulation results of cumulative distribution composed of two kinds of nearly mono-disperse particles (N_1=2000, N_2=200, one trial)

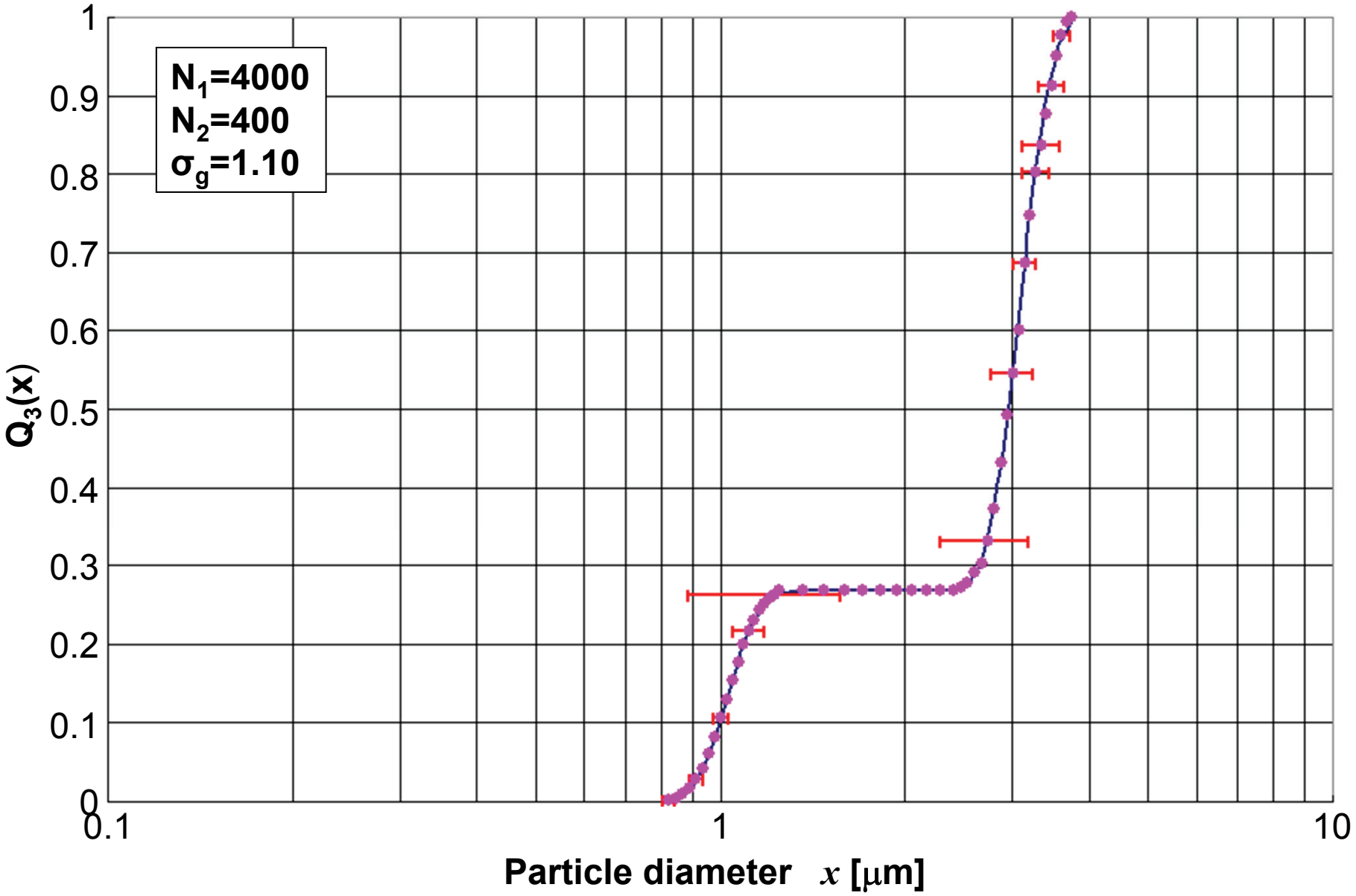

Fig.7 Simulation results of cumulative distribution composed of two kinds of nearly mono-disperse particles (N_1=4000, N_2=400, one trial)

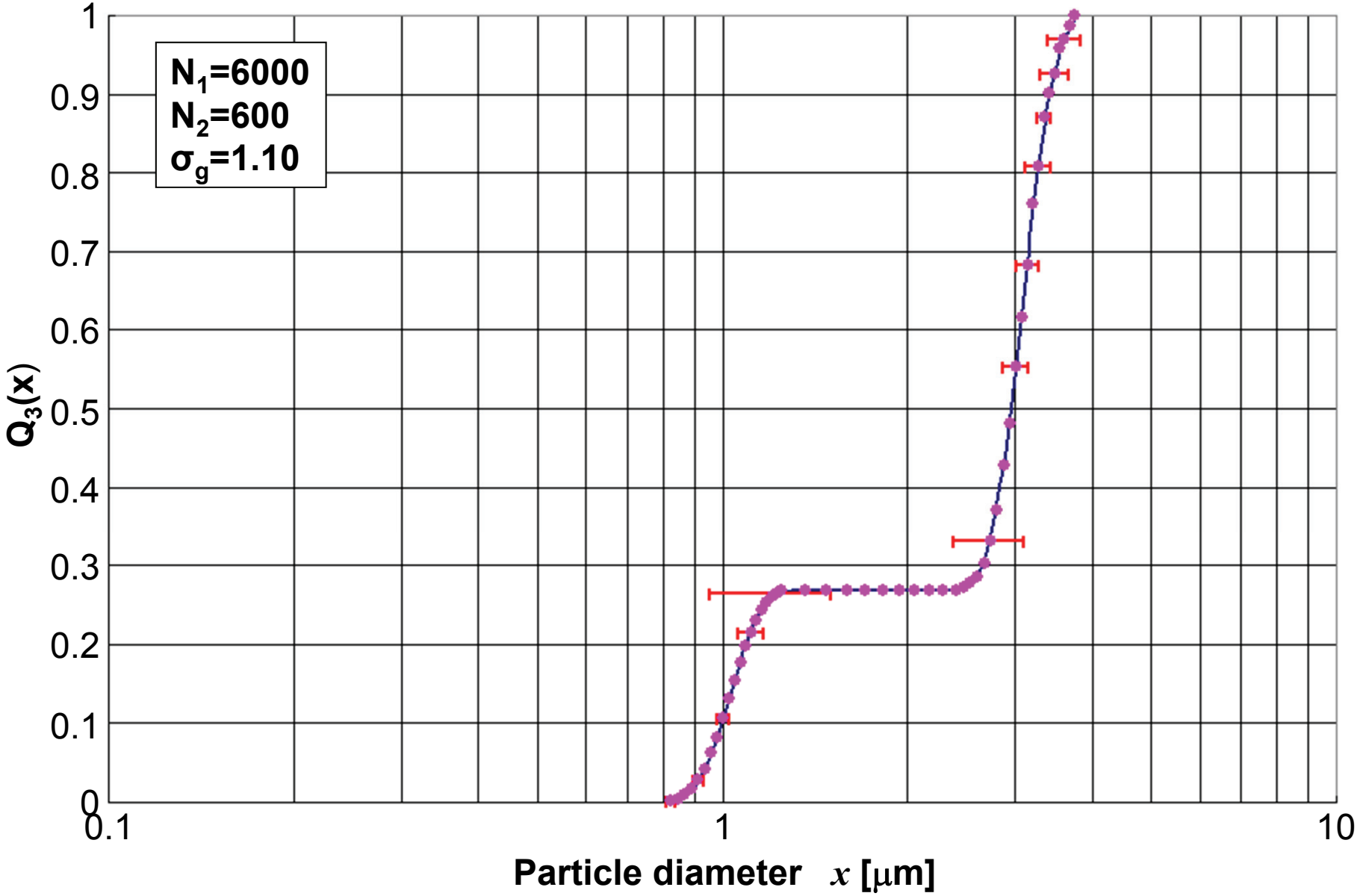

Fig.8 Simulation results of cumulative distribution composed of two kinds of nearly mono-disperse particles (N_1=6000, N_2=600, one trial)

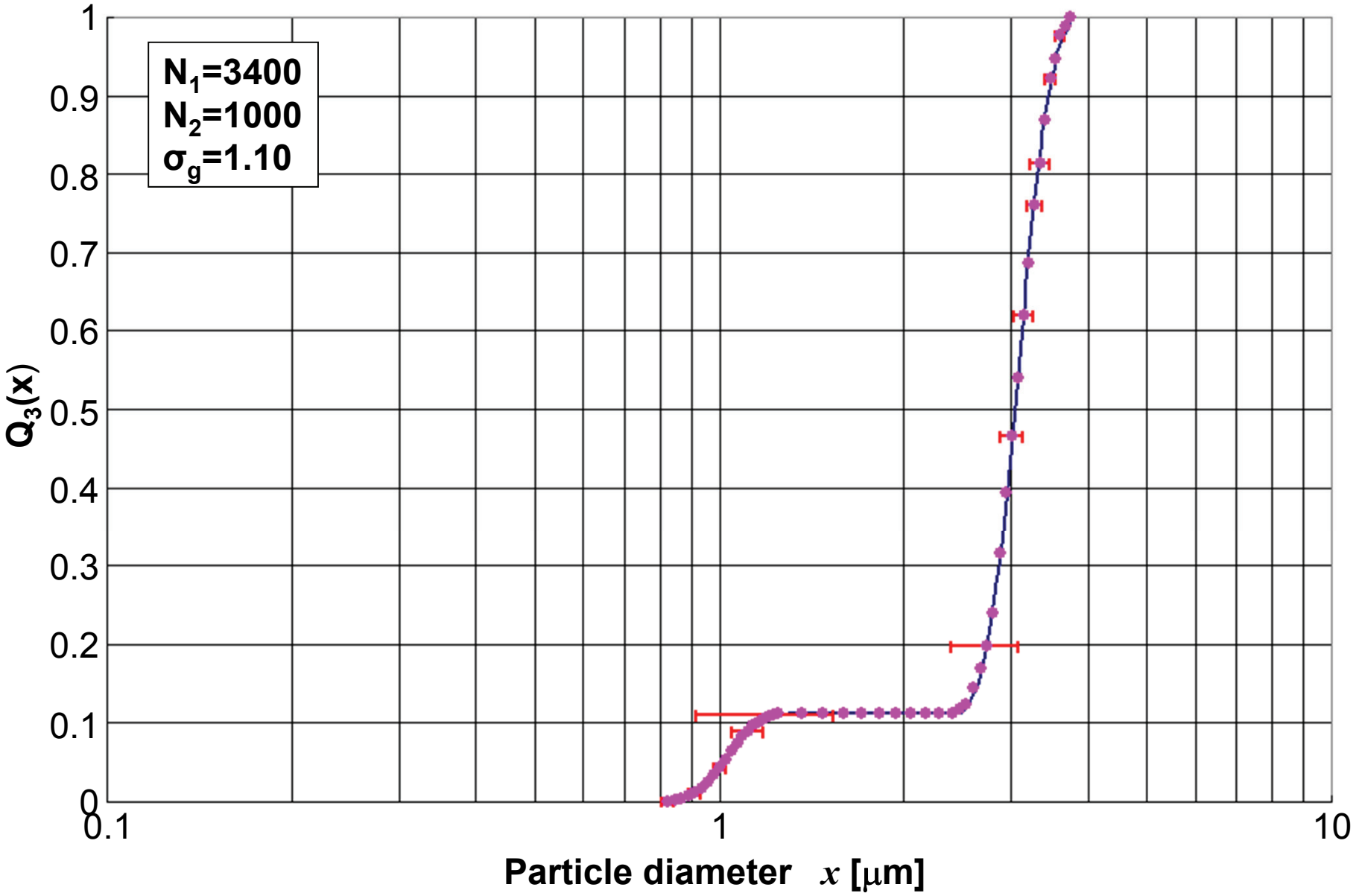

Fig.9 Simulation results of cumulative distribution composed of two kinds of nearly mono-disperse particles (N_1=3400, N_2=1000, one trial)

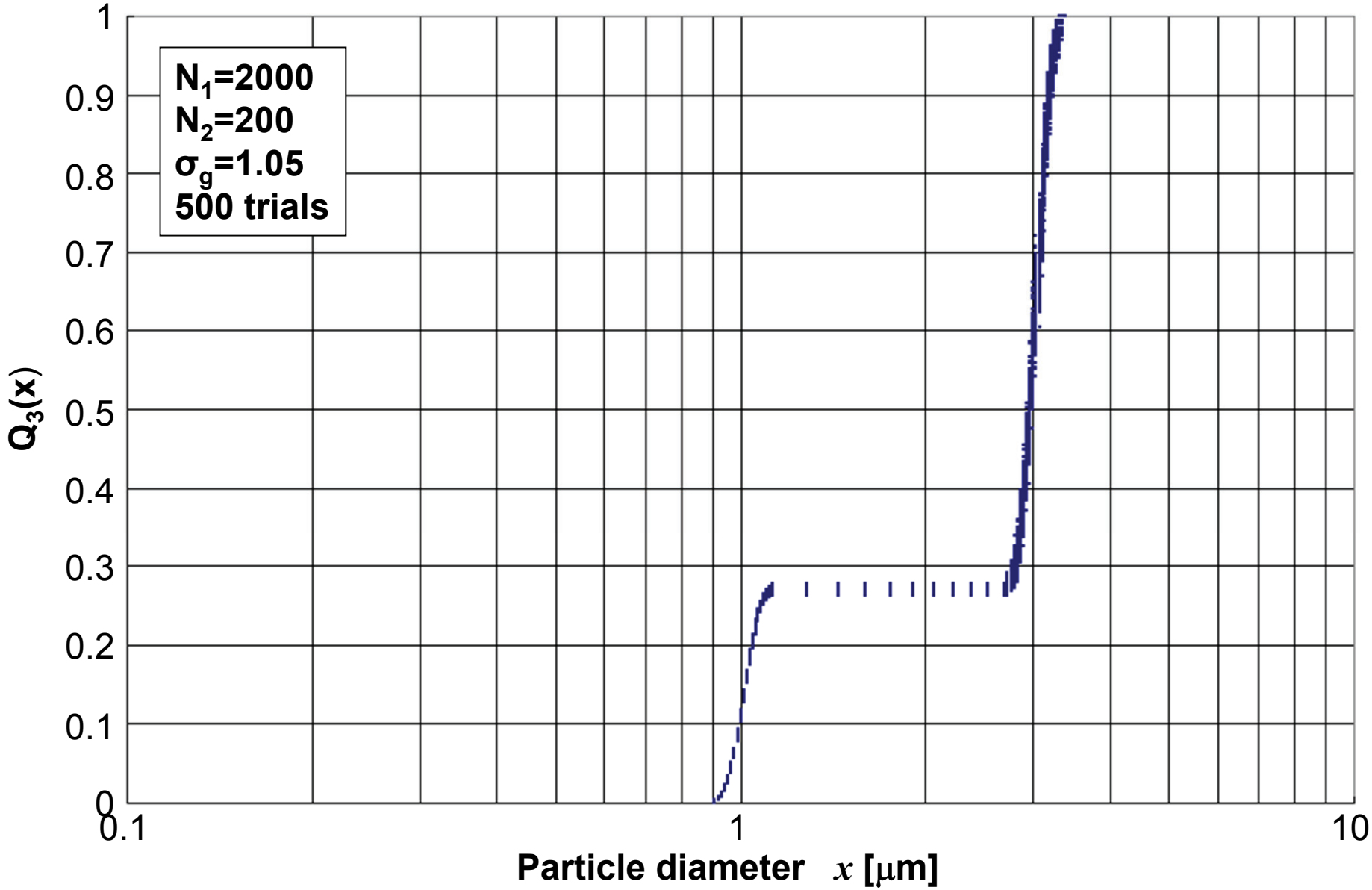

Fig.10 Simulation results of cumulative distribution composed of two kinds of nearly mono-disperse particles (N_1=2000, N_2=200, 500 trials, σ_g=1.05)

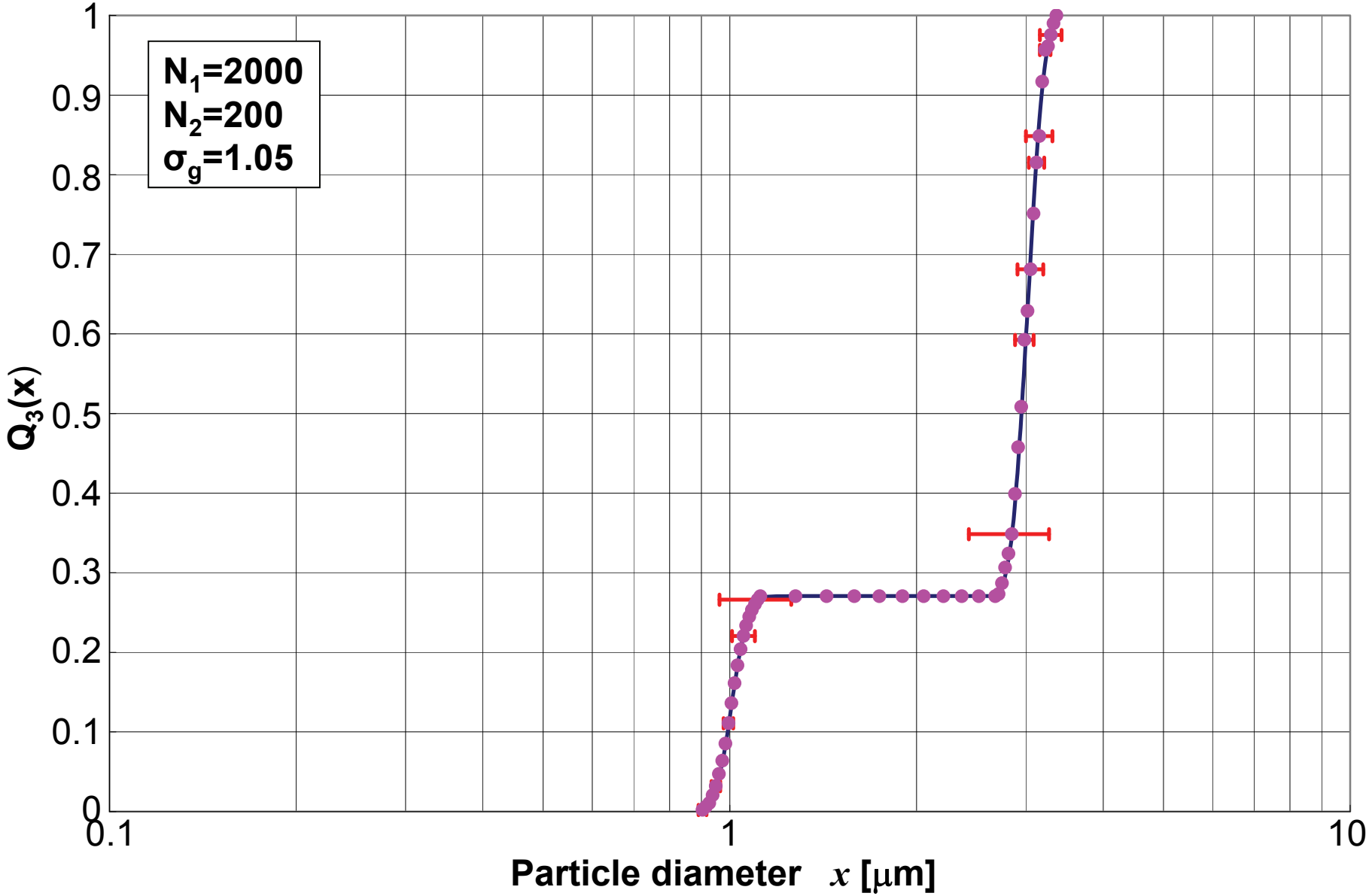

Fig.11 Simulation results of cumulative distribution composed of two kinds of nearly mono-disperse particles (N_1=2000, N_2=200, one trial, σ_g=1.05)